Erciyes Üniversitesi Veteriner Fakültesi Dergisi

Research Article
10.32707/ercivet.1847087

Imprint:
Volume: 23(1)
Year: 2026
Page: 31-47

Duygu YAMAN GRAM[a*]
Ayten KARABEKİR[b]
Ayhan ATASEVER[c]

[a] Asst. Prof., Erciyes University, dyamangram@gmail.com
[b] Master's Student, Erciyes University, ozvarola@gmail.com
[c] Emer. Prof., Erciyes University, ataseverayhan042@hotmail.com

[*] Corresponding Author

Received: 12/23/2025
Accepted: 3/26/2026

Citation:
Yaman Gram D, Karabekir A, Atasever A. The effects of L-arginine on Transforming Growth Factor Beta 1 (TGF-β1) expression and early renal alterations in streptozotocin-induced diabetic rats. Erciyes Univ Vet Fak Derg 2026;23(1), 31-47. https://doi.org/*10.32707/ercivet.1847087*

Screened by iThenticate for Authors & Researchers

The Effects of L-Arginine on Transforming Growth Factor Beta 1 (TGF-β1) Expression and Early Renal Alterations in Streptozotocin-Induced Diabetic Rats

Abstract

Diabetic nephropathy (DN) is a prevalent microvascular complication of diabetes mellitus, occurring in more than 40% of affected individuals, with reactive oxygen species–induced endothelial dysfunction playing a central role in its development. L-arginine may exert protective effects by interacting with these oxygen metabolites. This study investigated the effects of L-arginine on early renal changes in streptozotocin-induced diabetic rats. Additionally, renal levels and localization of transforming growth factor beta 1 (TGF-β1), an important fibrogenic factor involved in DN and endothelial-mesenchymal transition, were evaluated by ELISA and immunohistochemistry. Forty-eight male Wistar albino rats (250-300 g) were divided into four groups (n=12); control (0.1 mol/L sodium citrate buffer i.p.); L-arginine (100 mg/kg by gavage); STZ (50 mg/kg, i.p.); STZ+L-arginine (50 mg/kg STZ i.p.+ 100 mg/kg L-arginine by gavage). STZ was administered as a single dose, and L-arginine was given for twenty-one days. Histopathological examination of diabetic kidneys revealed glomerular enlargement, erythrocyte congestion in glomerular and interstitial vessels, cytoplasmic vacuolization in tubular epithelium, and hyaline deposition in glomeruli and tubules. TGF-β1 expression was detected in proximal and distal tubular epithelial cells and in the vascular media of all groups. However, TGF-β1 immunoreactivity was very mild in the control and L-arginine groups compared with the diabetes-induced groups. ELISA results confirmed significantly elevated renal TGF-β1 levels in diabetic rats, while L-arginine administration markedly reduced these increases. In conclusion, diabetes induced notable morphologic kidney alterations accompanied by increased TGF-β1 levels. L-arginine treatment attenuated TGF-β1 elevation, suggesting potential protective effects against diabetes-related renal vascular damage.

Keywords: Diabetes mellitus, kidney, L-arginine, rat, TGF-β1

Streptozotosin ile Diyabet Oluşturulmuş Ratlarda L-Arjinin'in Dönüştürücü Büyüme Faktör Beta 1 (TGF-β1) Ekspresyonu ve Erken Böbrek Değişiklikleri Üzerine Etkileri

Öz

Diyabetik nefropati (DN), diabetes mellitusun önemli bir mikrovasküler komplikasyonudur ve hastaların %40'ından fazlasını etkilemektedir. Reaktif oksijen türlerinin aracılık ettiği endotel disfonksiyonu DN'nin patogenezinde önemli bir rol oynamaktadır. L-arjinin, bu oksijen metabolitleri ile etkileşime girerek koruyucu etkiler gösterebilir. Bu çalışmada, streptozotosin (STZ) ile diyabet oluşturulmuş sıçanlarda L-arjininin erken böbrek değişiklikleri üzerindeki etkileri araştırılmıştır. Ayrıca, DN ve endotel-mezenkimal geçişte rol

oynayan önemli bir faktör olan transformasyon büyüme faktörü beta 1'in (TGF-β1) böbrek düzeyleri ve lokalizasyonu ELISA ve immünohistokimyasal yöntemlerle değerlendirilmiştir. Kırk sekiz erkek Wistar albino sıçan (250-300 g) dört gruba ayrılmıştır (n=12); kontrol (0,1 mol/L sodyum sitrat tamponu i.p.); L-arjinin (100 mg/kg gavaj yoluyla); STZ (50 mg/kg, i.p.); STZ+L-arjinin (50 mg/kg STZ i.p.+ 100 mg/kg L-arjinin gavaj yoluyla). STZ tek doz olarak, L-arjinin ise yirmi bir gün boyunca verildi. Diyabetik böbreklerin histopatolojik incelemesinde, glomerüler genişleme, glomerüler ve interstisyel damarlarda eritrosit birikimi, tübüler epitelde sitoplazmik vakuolizasyon ve glomerüllerde ve tübüllerde hiyalin birikimi görüldü. TGF-β1 ekspresyonu, tüm grupların proksimal ve distal tübüler epitel hücrelerinde ve vasküler medialarında tespit edildi. Bununla birlikte, TGF-β1 immünoreaktivitesi, diyabetli gruplara kıyasla kontrol ve L-arjinin gruplarında çok hafifti. ELISA ile diyabetik sıçanlarda böbrek TGF-β1 düzeylerinin önemli ölçüde yükseldiği, L-arjinin uygulamasının ise bu artışları belirgin şekilde azalttığı gözlendi. Sonuç olarak, STZ uygulaması, TGF-β1 düzeylerini artırarak belirgin morfolojik böbrek değişikliklerine neden oldu. L-arjinin tedavisi, artmış olan TGF-β1 düzeylerini azaltarak diyabetle ilişkili böbrek damar hasarına karşı olası koruyucu etkilerini düşündürdü.

Anahtar kelimeler: Böbrek, diabetes mellitus, L-arjinin, rat, TGF-β1

Introduction

Type 1 diabetes mellitus (T1DM) is a chronic metabolic disease characterised by insulin insufficiency and associated hyperglycaemia resulting from T-cell-mediated autoimmune or non-autoimmune destruction of pancreatic β cells (Yılmaz, 2006). According to the International Diabetes Federation (IDF), while the number of individuals with diabetes in the world is 589 million as of 2024, this number is estimated to reach 853 million in 2050 (IDF, 2025).The etiology of type 1 diabetes is quite complex and is still not fully understood. For this purpose, surgical (Müller, 2016), chemical (Rees and Alcolado, 2005; Szhudelski, 2001), viral (Ejrnaes et al., 2006), and genetic (Dedoussis et al., 2007) models are used in experimental diabetic animals. Among these methods, the most preferred are diabetes models using chemical agents. It is possible to induce diabetes using chemically produced diabetogenic agents such as alloxan or streptozotocin (STZ), both of which exhibit selective toxicity against pancreatic cells. STZ is more commonly preferred due to its greater β-cell specificity and lower off-target toxicity, whereas alloxan more readily induces severe hyperglycemia and ketosis (Küçük et al., 2012; Lenzen, 2008).

As one of the most severe complications of diabetes mellitus, diabetic nephropathy (DN), may lead to renal failure with decreased glomerular filtration as a result of albuminuria and increased blood pressure (Zhang et al., 2025). Early stages of DN are marked by vascular dysfunction and extracellular matrix accumulation in the kidney (Ziyadeh, 1993), which can contribute to renal hypertrophy, glomerular basement membrane thickening, and progressive glomerulosclerosis, ultimately leading to proteinuria and interstitial fibrosis in more advanced stages of disease (Yılmaz, 2006). Transforming growth factor-beta (TGF-β), a hypertrophic and pro-sclerotic cytokine that mainly stimulates hypertrophy of renal cells and overproduction of matrix proteins, has been shown to mediate almost all pathological changes in diabetic kidney disease (Ziyadeh et al., 1998). Studies have shown that TGF-β1 levels are increased in renal cells, including mesangial cells, and TGF-β1 upregulates ECM proteins such as collagens in DN (Kato et al., 2006; Reeves and Andreoli, 2000). Nitric oxide (NO), the most paradoxical molecule of oxidative stress, is a radical molecule due to the unpaired electron it carries. Nitric oxide, first identified as an endothelial-derived relaxation factor, is a key mediator of vascular homeostasis (Noris and Remuzzi, 1999). It has long been known that L-arginine, the precursor of nitric oxide, is one of the most critical factors stimulating insulin release (Szlas et al., 2022). The beneficial effects of L-arginine supplementation have been reported in urethral obstruction (Ito et al., 2005), puromycin-induced nephrosis (Reyes et al., 1994), diabetes-induced secondary nephropathy (Sadik, 2008), glomerular hypertension (Katoh et al., 1994), and various chronic kidney disease models (Klahr and Morrissey, 2004). In both in vitro and in vivo studies, beneficial effects of L-arginine administration on the endothelium have been observed in various diabetes models (Pieper and Peltier, 1995). It has also been reported that L-arginine reduces oxidative stress by improving endothelial function by reducing vascular superoxide production in hypercholesterolemic humans (Kawano et al., 2002). Therefore, this study aimed to determine the effects of L-arginine on the renal tissue level of

TGF-β1 and its localisation and early renal changes in streptozotocin-induced diabetic rats.

Materials and Methods

Streptozotocin and L-Arginine

STZ (Cat. No S0130) and L-arginine (Cat. No A5006) were obtained from Sigma-Aldrich, Germany.

Animals

The material used in this study consists of kidney tissues obtained from rats in which diabetes was experimentally induced in our previous experiment (Yaman Gram et al., 2025). Briefly, a total number of 48 male Wistar albino rats (250-300 g body weight) were obtained from Erciyes University Experimental Research and Application Center. The animals were housed in polycarbonate cages (3 rats in each cage) and were kept in a special room at a constant temperature 22°C±2°C and humidity (50%±5%) with 12-h light/dark cycles and had free access to diet and tap water. The experiments were carried out in accordance with the Guidelines for Animal Experimentation approved by Erciyes University (dated 11.01.2018 and decision no:18/017).

Induction of DM

The animals were fasted for 12 hours before the induction of diabetes. STZ, freshly prepared in citrate buffer (0.1 M, pH 4.5), was injected into rats as a single dose of 50 mg/kg intraperitoneally (i.p.). At 72 hours after the injection, diabetes was verified by checking the fasting blood glucose levels using a glucometer (Gram Yaman et al., 2025). While blood glucose levels were measured as 104.82±1.59 mg/dL in control rats, they were 407.58±24.45 mg/dL in diabetic rats (Yaman Gram et al., 2025). Rats with blood glucose levels above 200 mg/dL were considered diabetic and included in the study (Cakir et al., 2018; Kaya et al., 2022).

Experimental design

Rats were divided equally into four groups as follows: Control group: rats were only injected with citrate buffer (0.1 ml., pH 4.5) body weight/day (b.w./day). L-arginine group: Rats received L-arginine (100 mg/kg b.w./day) daily for 21 days. STZ group: Rats injected with a single dose of STZ (50 mg/kg b.w./day). STZ+L-arginine group: Rats were given L-arginine (100 mg/kg b.w./day) starting 3 days after a single dose of STZ (50 mg/kg b.w./day). L-arginine was dissolved in PBS and administered by intragastric gavage daily for 21 days. The animals were given feed and water ad libitum. Doses of L-arginine (El-Missiry et al., 2004) and STZ (Cakir et al., 2018; Kaya et al., 2022) used in the study were determined according to the results of previous studies. Blood glucose levels were measured weekly on the 7th, 14th, and 21st days to control diabetes status.

Collection and Preparation of Samples

24 hours after the last L-arginine administration, rats were anesthetized with an intramuscular injection of 80 mg/kg Ketamine (Alfamine, 100 mg/mL) and 12 mg/kg Xylazine (Alfazyne, 20 mg/mL). Both were purchased from Ata-Fen. All the animals were sacrificed, then one kidney was placed and fixed in neutral-buffered formalin (10%). Dehydration of the kidney samples was performed in a graded ethanol series. Kidney samples were cleared in xylene. Then they were embedded in paraffin for the histopathological examination [Hematoxylin-Eosin (H&E), Periodic-acid-Schiff (PAS), and Crossmon's triple stainings and immunohistochemistry techniques], and the other one was kept at -80 °C for further analysis.

Histopathological Analysis

A rotary microtome was used for cutting the kidney tissues at 5µm thickness. They were mounted on Epredia SuperFrost Plus Adhesion slides (Epredia, Microm International GmbH, Germany). Deparaffinization was achieved in xylene, and then they were rehydrated. H&E stain (Luna, 1968) was used for general histopathological examination. Crossmon's triple stain (Crossmon, 1937)

was used to demonstrate collagen fibers, and PAS stain (Bancroft and Cook, 1984) was used to evaluate basement membrane thickness, as described previously. Microscopic evaluation was conducted using an Olympus BX51 microscope (Olympus Europa SE and Co., Hamburg, Germany).

Immunohistochemical Assessment of TGF-β1

Localization of TGF-β1 expression in kidney tissues, was performed according to the previously published procedure (Gram et al., 2019). First, formalin-fixed, paraffin-embedded kidney tissue samples were cut to a thickness of 4-5 μm using a microtome. Sections were immersed in xylene for deparaffinization. A graded ethanol series was used for rehydration of the tissue samples. Then, the samples were placed in a 10 mM, pH 6.0 citrate buffer and heated in a microwave oven at 600W for 15 minutes to facilitate antigen retrieval. Then, the endogenous peroxide activity of the slides was blocked in 0.3% hydrogen peroxide in methanol for 30 min. Nonspecific antibody binding was reduced by treating tissue samples with normal goat serum. Samples were then incubated with the primary antibody. Rabbit polyclonal anti-TGF-β1 (Sigma-Aldrich, SAB4502954) was used as the primary antibody (1:100 dilution). Antibody dilution was performed using IHC buffer (0.8 mM Na2HPO4, 1.47 mM KH2PO4, 2.68 mM KCl, 137 mM NaCl) containing 0.3% Triton X (pH 7.2-7.4). As an isotype control, sections were incubated with non-immune IgG of the same species from which the primary antibody was made, and the concentration of IgG was the same as the protein concentration of the primary antibody. As a negative control, slides were incubated with PBS (pH 7.4) instead of the primary antibody. Following overnight primary antibody incubation at +4°C, IHC buffer was used to wash sections. The tissue samples were then incubated with a biotinylated secondary antibody. Biotinylated goat anti-rabbit IgG (Vector Laboratories Inc., BA-100) was used as the secondary antibody (1:100 dilution). The sections were treated with the Vectastain ABC kit (Vector Laboratories Inc.) according to the manufacturer's instructions. Liquid DAB+ substrate kit (Agilent Dako, Santa Clara, CA, USA) was used to visualize the peroxide activity. Mayer's hematoxylin was used to counterstain the sections. Then the samples were washed under tap water. Next, dehydration of sections was achieved in a graded ethanol series and then covered with Entellan®.

Morphometric Analysis of the Kidney

For morphometric analysis from all groups, comparison of glomerular and Malpighian corpuscle diameters in kidney sections was performed using a previously published protocol (Tarladacalisir et al., 2008). A total of 100 glomeruli (10 rats x 10 glomeruli) representing each group were evaluated. The diameters of each glomerulus and Malpighian corpuscle were measured under a light microscope (at a magnification of 20x, (Olympus BX51) by using ImageJ software (Schneider et al., 2012). For each glomerulus, two diameters, the greatest and the smallest, were measured. Based on these measurements, the average glomerular diameter was calculated.

Biochemical Analysis

According to the manufacturer's instructions, the kidney tissue TGF-β1 levels were determined in an ELISA device (BioTek, uQuant) using a rat-specific commercially available ELISA kit (Sun Red Bio, Catalog No: 201-11-0780). For this purpose, all reagents and samples were used at room temperature (18-25°C). 50 μL standard + 50 μL streptavidin HRP was added to each of the wells designated as standard, and 40 μL sample + 10 μL TGF-β1 antibody + 50 μL streptavidin HRP was added to each of the wells designated as sample according to the manufacturer's instructions. The ELISA plate was then covered and incubated at 37°C for 60 minutes. Immediately after incubation, the mixtures in the wells were removed. Subsequently, each well was washed with 350 μL of washing solution for 1-2 min. Then the washing solution was discarded. After repeating the washing process 5 times, the plate was blotted dry on a clean blotting paper. After adding 50 μL of chromogen A + 50 μL of chromogen B to each well, the plate was covered and placed in an incubator at 37°C for 10 minutes. Then, 50 μL of stop solution was added to each well. Measurement of the plate was performed spectrophotometrically at a wavelength of 450nm±2nm. The concentration of TGF-β1 in the sample was then determined by comparing the sample's optical density (OD) with the standard OD curve. The estimated mean was 64.63 with a 95% confidence interval of 63.77-65.50.

Statistical Analysis

The data obtained were normally distributed based on the Kolmogorov-Smirnov and Shapiro-Wilk tests. Homogeneity of variances was confirmed using Levene's test. Therefore, parametric one-way analysis of variance (ANOVA) was performed for global comparison to evaluate the effects of STZ and L-arginine treatment on kidney TGF-β1 levels, glomerular and Malpighian corpuscle diameters. SPSS version 24 (IBM) was used for statistical analyses. In the case of statistically significant differences ($P<0.05$), the Tukey- Kramer multiple comparisons post-test was applied. The data are presented as the mean ± s.d. The level of significance was set at $P<0.05$.

Results

Effects of STZ and L-arginine Treatment on Kidney Histopathology

Histopathological examination of kidney tissues in the control (Figure 1A) and in the L-arginine group (Figure 1B) showed normal renal cortical structure, including numerous renal corpuscles (Malpighian corpuscles), proximal tubules, and distal tubules. The cuboidal epithelial cells of the proximal tubules with a well-developed brush border of microvilli appeared normal with acidophilic cytoplasm. Distal tubules, which were recognized by basophilic staining and the absence of a brush border, had wider lumens than proximal ones. Examination of the H&E-stained kidney sections from the STZ group revealed marked glomerular enlargement within the cortical region. The hypertrophic glomeruli were closely apposed to the parietal layer of Bowman's capsule, resulting in a pronounced reduction of Bowman's space. Tubular epithelial cells in the cortex exhibited cytoplasmic vacuolization, indicating cellular degeneration (Figure 1C). Similarly, in the STZ + L-arginine group, glomerular enlargement was comparable to that in the STZ group, and epithelial cells of both proximal and distal tubules showed cytoplasmic vacuolization (Figure 1D). Moreover, numerous hyaline casts were present within the lumens of proximal tubules in the STZ group (Figure 2A). In addition, capillaries of the glomeruli and interstitial vessels contained dense aggregates of erythrocytes (Figure 2B).

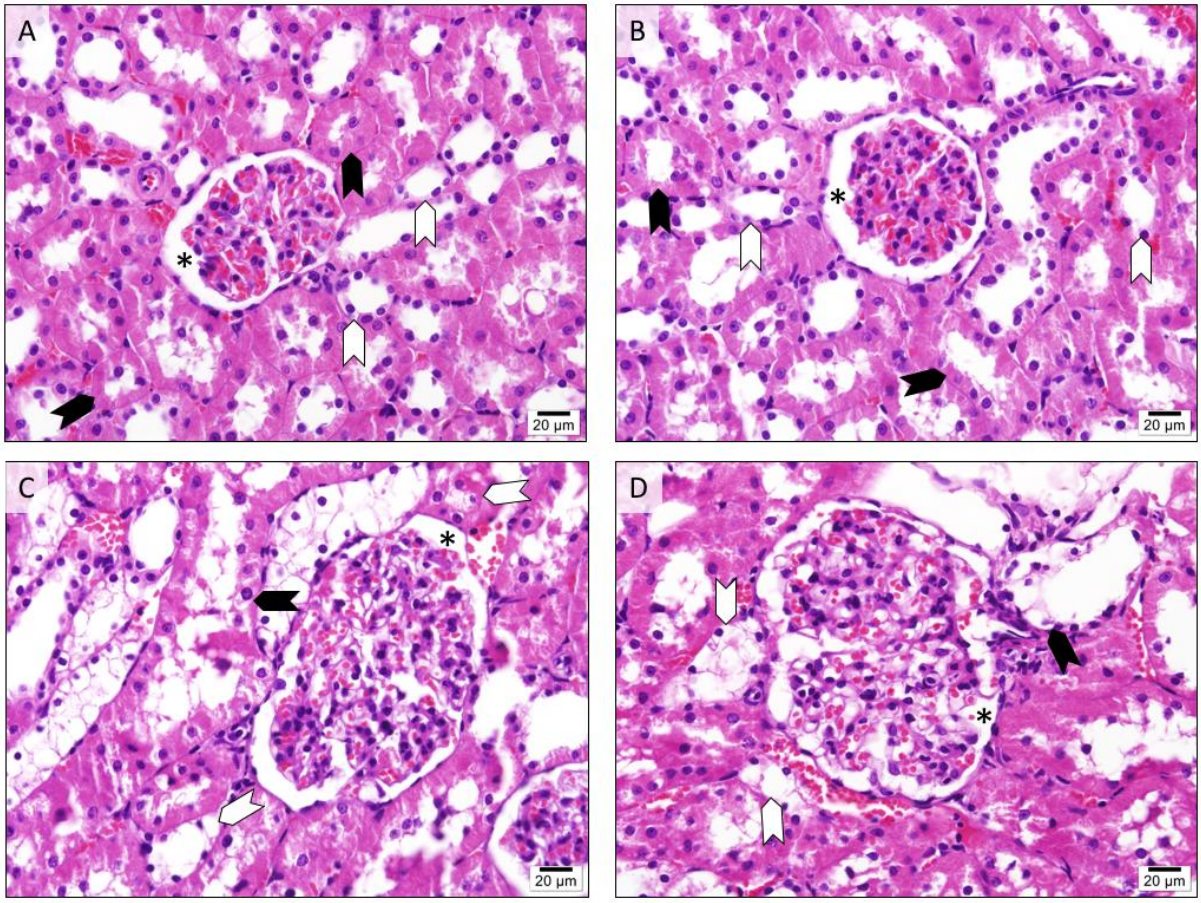

Figure 1. Renal cortical tissue in the Control (A) and L-arginine (B) groups exhibited normal histological architecture, characterized by numerous renal corpuscles, clearly distinguishable proximal tubules (black arrowhead) and distal tubules (white arrowhead), as well as Bowman's space (asterisk). In the STZ (C) and STZ + L-arginine (D) groups, histopathological alterations were observed in the renal cortex, including glomerular hypertrophy, narrowing of Bowman's space (asterisk), and cytoplasmic vacuolization within the epithelial cells of both distal (white arrowhead) and proximal (black arrowhead) tubules, H&E-staining.

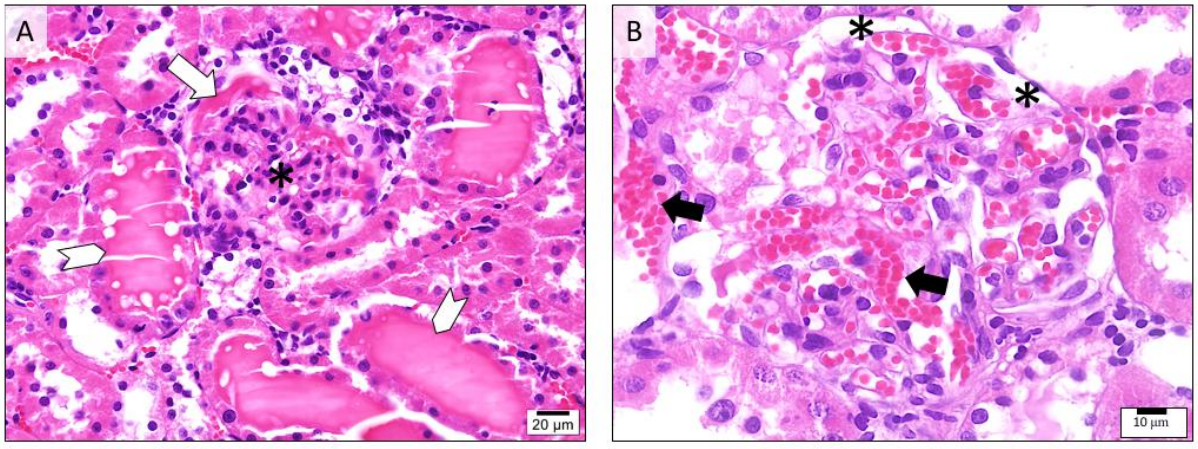

Figure 2. Kidney sections from the STZ group revealed marked glomerular enlargement in the renal cortex (star). Numerous hyaline casts were observed within the lumens of the proximal tubules (white arrowhead) and glomeruli (white arrow) (A). Glomerular enlargement was accompanied by narrowing of Bowman's space (star). Additionally, there was erythrocyte stasis in glomerular capillaries and interstitial blood vessels (black arrow) (B), H&E-staining.

Crossmon's trichrome-stained kidney sections from the control (Figure 3A) and L-arginine (Figure 3B) groups displayed normal cortical architecture, characterized by well-defined Malpighian corpuscles and intact proximal and distal tubules, consistent with observations obtained from H&E staining. In contrast, sections from the STZ (Figure 3C) and STZ + L-arginine (Figure 3D) groups exhibited marked pathological alterations, including pronounced glomerular enlargement, narrowing of Bowman's space, and thickening of the parietal layer of Bowman's capsule attributable to increased connective tissue deposition. Connective tissue expansion was also evident within the mesangial regions.

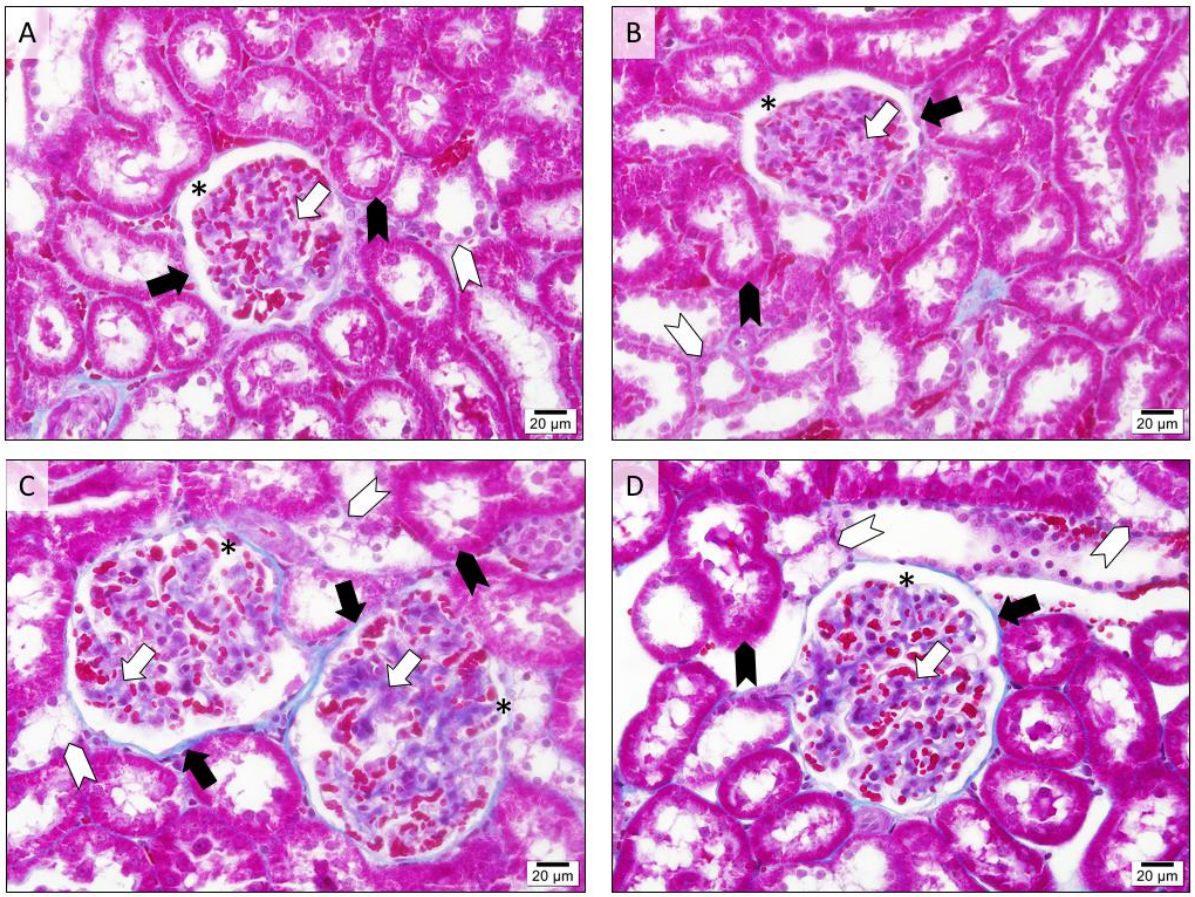

Figure 3. Kidney sections from the Control (A) and L-arginine (B) groups exhibited normal renal cortical architecture, including numerous renal corpuscles, intact proximal (black arrowhead) and distal tubules (white arrowhead), normal mesangial matrix (white arrow), an unaltered parietal layer of Bowman's capsule (black arrow), and a clearly defined Bowman's space (asterisk). In contrast, the STZ (C) and STZ + L-arginine (D) groups showed thickening of the parietal layer of Bowman's capsule (black arrow) and increased deposition of mesangial matrix (white arrow), indicative of connective tissue accumulation. Additionally, these groups exhibited narrowed Bowman's space (star) and cytoplasmic vacuolization in proximal (black arrowhead) and distal (white arrowhead) tubular epithelial cells, Crossmon's triple staining.

Periodic acid–Schiff (PAS) staining was utilized to evaluate the thickness of basement membranes within renal tubules and glomerular capillaries (Figure 4A-D). In the control (Figure 4A) and L-arginine-treated groups (Figure 4B), PAS-positive staining was observed along the basement membranes of renal tubules, glomerular capillaries, and the parietal layer of Bowman's capsule, reflecting normal histoarchitecture. In contrast, kidney sections from the STZ-induced diabetic group (Figure 4C) exhibited intense PAS positivity in the glomerular capillary basement membranes, accompanied by increased mesangial matrix and enhanced mesangial cell proliferation. Additionally, PAS-positive granular structures consistent with phagosomes were identified within the cytoplasm of epithelial cells in both proximal and distal tubules. Similar pathological alterations were evident in the

STZ + L-arginine-treated group (Figure 4D), including prominent cytoplasmic phagosomes in tubular epithelial cells, as confirmed under higher magnification.

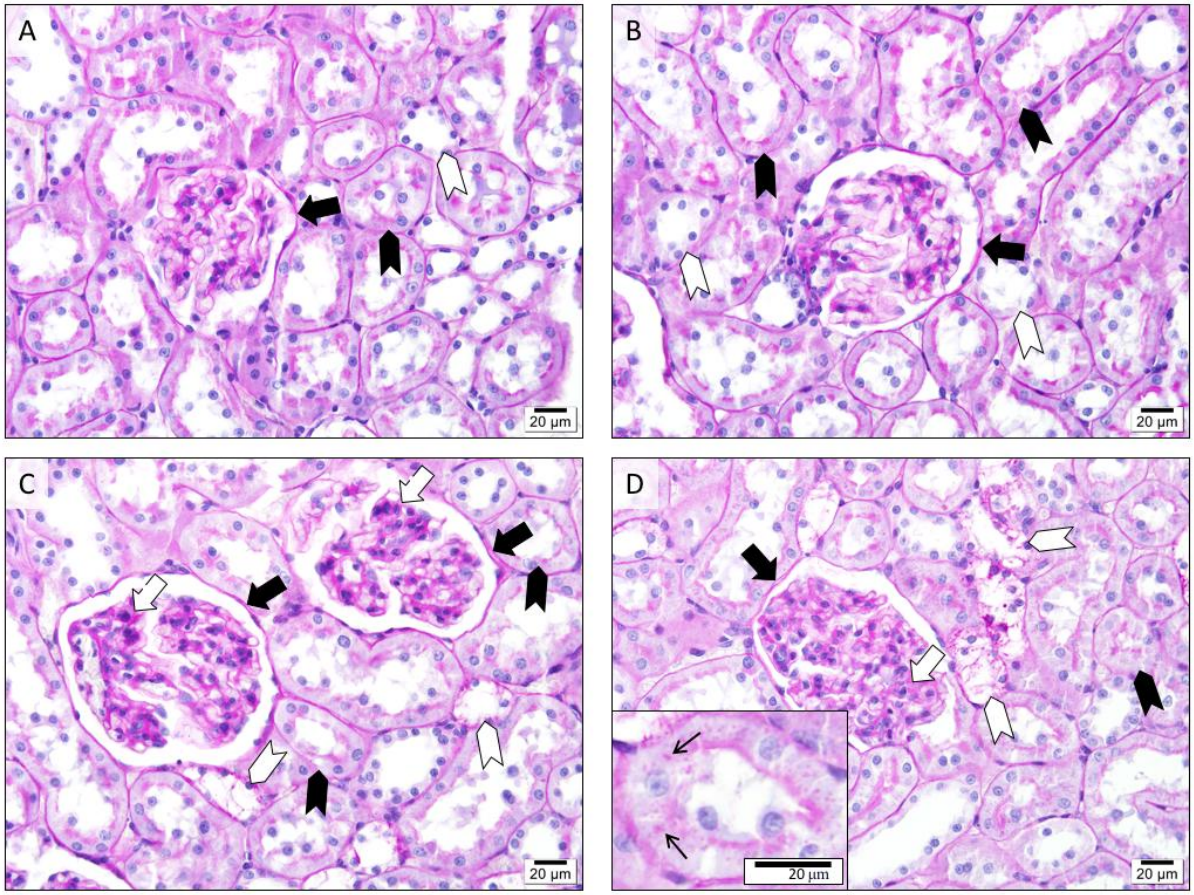

Figure 4. PAS staining of kidney sections from the Control (A) and L-arginine (B) groups revealed positive staining of the basement membranes of proximal tubules (black arrowhead), distal tubules (white arrowhead), glomerular capillaries, and the parietal layer of Bowman's capsule (black arrow), indicating preserved structural integrity. In the STZ (C) and STZ + L-arginine (D) groups, PAS staining revealed thickening of the parietal layer of Bowman's capsule (black arrow) due to increased connective tissue. Enhanced mesangial matrix deposition was also evident (white arrow). Tubular injury was characterized by cytoplasmic vacuolization in the epithelial cells of distal (white arrowhead) and proximal (black arrowhead) tubules. Additionally, PAS-positive phagosome-like granular structures were detected in the cytoplasm of some proximal and distal tubular epithelial cells (thin arrows, high magnification in D).

Effects of STZ and L-arginine Treatment on Glomerular and Malpighian Corpuscle Diameters

Light microscopic evaluation demonstrated a significant increase in glomerular diameters in both the STZ and STZ + L-arginine groups compared with the control and L-arginine groups ($P<0.001$ for both comparisons). However, there was no statistically significant differences among the groups in terms of Malpighian corpuscle diameter ($P>0.05$). Additionally, comparison between the STZ and STZ + L-arginine groups revealed no significant difference in Malpighian corpuscle dimensions (Figure 5).

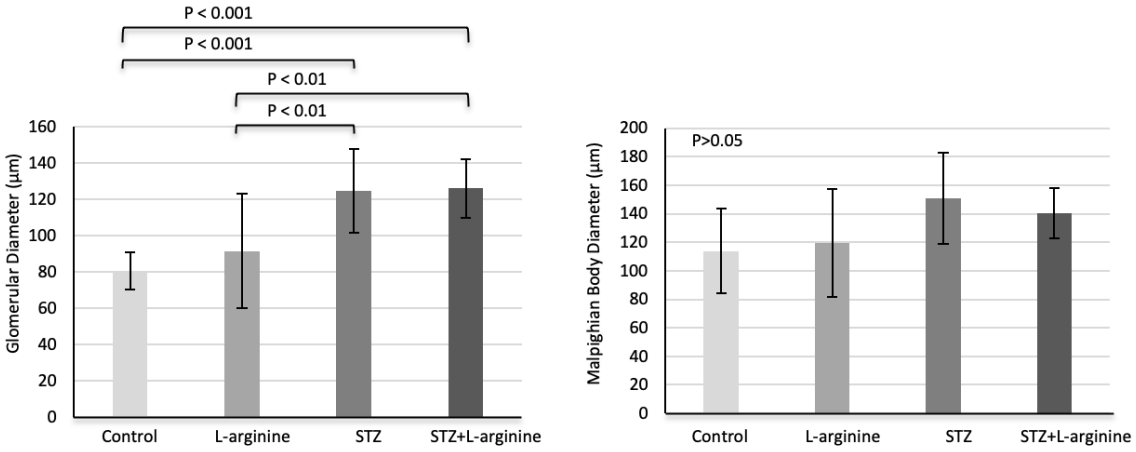

Figure 5. Evaluation of glomerular and renal corpuscle (Malpighian body) diameters in control and experimental groups (µm)

Localization of TGF-β1 in Kidney Samples

TGF-β1 immunoreactivity was observed in renal tissue across all experimental groups (Figure 6A-D). In the control (Figure 6A) and L-arginine (Figure 6B) groups, strong TGF-β1 immunolabeling was primarly localized to the vascular media. Prominent immunoreactivity was also observed in the epithelial cells of the proximal tubules, whereas labeling in the distal tubules was minimal. In contrast, kidney sections from the STZ group showed a broader distribution of TGF-β1, with immunolabeling present in the vascular media, proximal and distal tubules, and mesangium (Figure 6C). Furthermore, L-arginine treatment did not cause any differences in the intensity of the TGF-β1 expression associated with diabetes (Figure 6D).

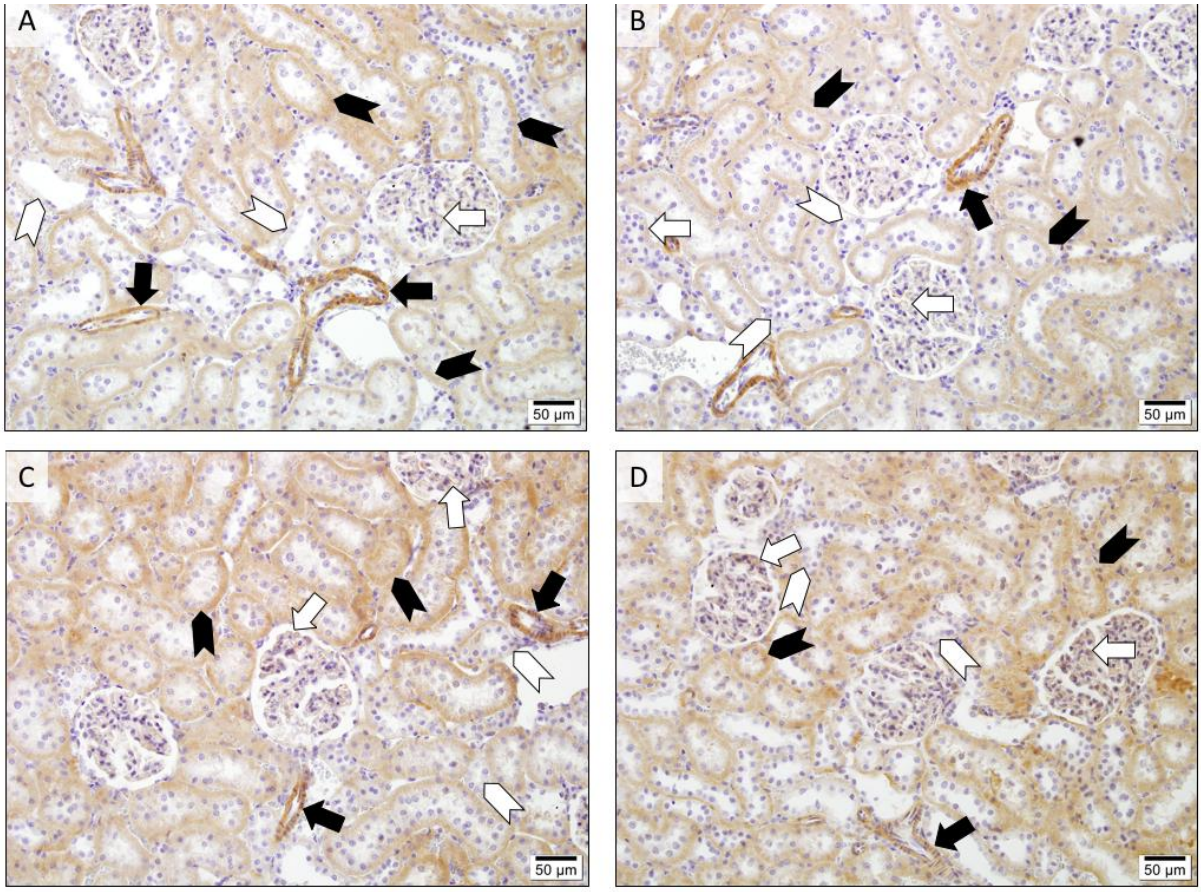

Figure 6. TGF-β1 immunoreactivity was detected in kidney tissues across all groups. In the Control (A) and L-arginine (B) groups, strong TGF-β1 expression was observed predominantly in the media layer of renal vessels (black arrow). TGF-β1 was also immunolocalized in the proximal tubules (black arrowhead). Low expression for TGF-β1 was observed in the distal tubules (white arrowhead). In the STZ-induced diabetes (C) and STZ + L-arginine (D) groups, TGF-β1 immunoreactivity was more prominent, localized in the proximal (black arrowhead) and distal tubules (white arrowhead), mesangial region (white arrow), and the media layer of the vessels (black arrow).

Effects of STZ and L-arginine Treatment on TGF-β1 Expression in the Kidney

No significant difference in renal TGF-β1 levels was observed between the control and L-arginine groups. In contrast, the STZ-treated group, renal TGF-β1 levels increased significantly compared to the control group ($P<0.05$). Administration of L-arginine to diabetic rats resulted in a significant reduction in TGF-β1 levels, with values approaching those observed in the control group (Figure 7).

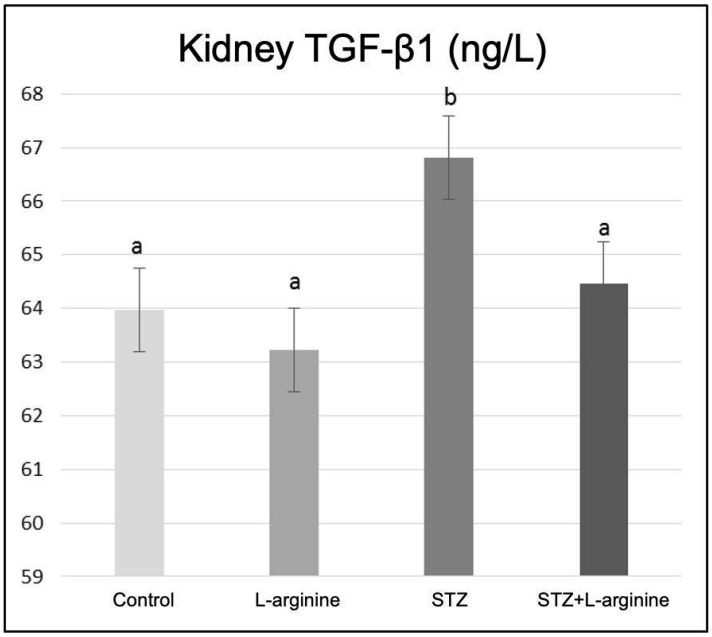

Figure 7. TGF-β1 concentrations in renal tissue of rats in control and experimental groups (ng/L)

Discussion and Conclusion

Diabetic nephropathy is one of the reasons for end-stage renal disease all over the World. Furthermore, it is also a significant cause of morbidity and mortality in patients with Type 1 and Type 2 diabetes (Hoogeveen, 2022). While diabetic nephropathy typically refers to advanced renal damage characterized by progressive albuminuria, hypertension, and reduced glomerular filtration rate (Yang and Xu, 2022), this study focuses on the early renal changes. The pathophysiological mechanisms underlying the development of diabetic nephropathy are multifactorial. Hyperglycemia is recognized as the primary initiating factor, triggering glomerular hyperfiltration and microalbuminuria, which are followed by glomerular hypertrophy, progressive mesangial matrix expansion, tubulointerstitial fibrosis, and ultimately, glomerulosclerosis and end-stage renal disease (Koszegi et al., 2022).

To enhance understanding of the pathophysiology of DM, various diabetogenic agents such as STZ (Cakir et al., 2018; Roy et al., 2016; You et al., 2014) and alloxan (Ajiboye et al., 2020; Mistry et al., 2023) are widely employed in experimental animal models. In the present study, a single intraperitoneal dose of 50 mg/kg STZ, whose diabetogenic mechanism is well characterized, was administered to induce an experimental model of diabetes (Cakir et al., 2018; Kaya et al., 2022). Blood glucose levels were measured after 72 hours post-STZ administration, and animals with levels exceeding 200 mg/dL were classified as diabetic. The most commonly reported pathological alterations in diabetic kidneys include cellular vacuolization, pyknotic nuclei, medullary congestion, hemorrhagic and hyaline cast deposits, apical blistering, glomerular hypertrophy, dilated and congested glomerular capillaries, and fragmentation of tubular epithelial cells (Adeva Andany et al., 2023; Palsamy and Subramanian, 2011). In the present study, consistent with the literature, Malpighian corpuscles in the cortical region of kidneys from control rats exhibited normal histological architecture. In contrast, kidneys from the diabetic group demonstrated glomerular hypertrophy accompanied by a reduction in Bowman's space, which is attributable to the enlarged glomeruli. This glomerular enlargement is likely the result of increased cell number and volume, as well as dysregulation of mesangial cell proliferation.

Quantitative analysis of glomerular and Malpighian corpuscle dimensions using ImageJ software revealed a significant increase in glomerular diameter in the diabetic groups compared to the control groups. The observation of narrowing of Bowman's space suggests an increase in both the number and

volume of mesangial cells. Consistently, Crossmon's triple staining demonstrated thickening of the parietal layer of Bowman's capsule in the STZ group, attributable to increased connective tissue deposition, accompanied by a corresponding expansion of connective tissue within the mesangium. Additionally, PAS staining demonstrated an increase in mesangial cells within the glomerular capillary basement membranes in kidneys from STZ-treated rats. PAS-positive granular structures were also observed in the cytoplasm of epithelial cells in both proximal and distal tubules. These PAS-positive, phagosome-like particles likely reflect enhanced phagocytic activity associated with the clearance of degenerated tubular epithelial cell debris.

In addition, stasis observed in glomerulus capillaries and interstitium vessels in diabetic kidney tissues suggests distruption in microvascular function in T1DM. However, the precise mechanisms contributing to endothelial damage in T1DM remain insufficiently defined. L-arginine, the precursor for NO synthesis via nitric oxide synthase (NOS), is essential for regulating kidney function (Saleh and El-Demerdash, 2005). Since NO plays a critical role in the regulation of renal blood flow, glomerular filtration rate, and renin and angiotensin reabsorption and overall renal homeostasis, decreased NO bioavailability is thought to be an essential factor in DN (Chen et al., 1992). Consistently, reduced endothelial nitric oxide synthase (eNOS) expression has been reported to exacerbate DN (Wang et al., 2011). Since diminished L-arginine bioavailability is closely linked to impaired eNOS activity, L-arginine supplementation helps prevent endothelial dysfunction by addressing this deficiency. For this purpose, in the present study, L-arginine was administered via gavage to evaluate its potential protective effects against endothelial dysfunction in diabetic rats. No histopathological alterations were observed in the glomeruli and tubules of the kidneys of rats administered only L-arginine, suggesting that L-arginine does not exert adverse effects on renal morphology. However, in the experimental diabetes group induced by a single 50 mg/kg dose of STZ, L-arginine supplementation at the same dose used in the control group did not alter STZ-induced type 1 diabetes-associated renal damage based on histopathological assessment. Consistent with our findings, You et al. (2014) reported that although long-term L-arginine supplementation in drinking water effectively elevated circulating and renal L-arginine levels in type 1 diabetic mice, it did not lead to improvements in histological changes associated with type 1 diabetes. L-arginine did not significantly affect the histopathological alterations associated with renal damage, potentially due to compromised cellular uptake of L-arginine, particularly in eNOS-expressing renal cells. Consequently, further detailed molecular investigations, including evaluation of renal eNOS expression levels in STZ-induced type 1 diabetic rats, will enhance our understanding of the mechanisms underlying type 1 diabetes-mediated renal pathology.

Dysregulation of the TGF-β pathway, particularly TGF-β1, is recognized as a key contributor to the development and progression of T1DM complications (Heydarpour et al., 2020). Studies have shown that TGF-β1 levels are increased in the kidneys of animals with T1DM in both the early and late stages of the disease (Hill et al., 2000; Sharma and Ziyadeh, 1994). In a recent study, L-arginine was demonstrated to effectively modulate the fibrotic response and reduce profibrotic factor levels in the testes of diabetic rats (Sayed et al., 2023). Additionally, it has been reported that the TGF-β signaling pathway is involved in mediating diabetes-induced inflammatory and fibrotic alterations in the lung (Talakatta et al., 2018). In the present study, we investigated the effects of L-arginine on TGF-β1 localization and renal tissue levels in STZ induced diabetic rats. Our results revealed that in both control and L-arginine-treated non-diabetic groups, TGF-β1 immunoreactivity was primarily localized to the vascular media of renal blood vessels and to the epithelial cells of the proximal tubules, while distal tubules exhibited minimal expression. In contrast, diabetic rats displayed more intense renal TGF-β1 immunoreactivity compared with controls. Additionally, its localization was observed in the glomerular mesangium. Similarly, these findings are consistent with previous reports indicating that experimental diabetes induced with 50 mg/kg STZ in male Wistar rats leads to elevated TGF-β1 expression in the kidney, particularly within the glomeruli and mesangial regions (Roy et al., 2016).

Furthermore, our study demonstrated that renal TGF-β1 levels were high in diabetic rats. The increase in TGF-β1, a key profibrotic cytokine, suggests enhanced mesangial cell activation and expansion of mesangial matrix, likely due to excessive production and deposition of extracellular

matrix proteins. Dietary L-arginine supplementation has been shown to recover renal hemodynamics and reduce matrix expansion in various models of hypertensive kidney disease (Noris and Remuzzi, 1999). These effects have been attributed to increased endogenous NO production, suggesting that dietary L-arginine may enhance NO synthesis. However, limited studies have specifically investigated the potential protective effects of L-arginine on renal tissue in experimentally induced diabetes. Therefore, the present study provides valuable insight into the possible renoprotective role of L-arginine in STZ-induced diabetic rats.

In the kidneys of diabetic rats treated with L-arginine, TGF-β1 was strongly immunolocalized in mesangial cells, the vascular media, and both proximal and distal tubules, exhibiting a pattern similar to that observed in untreated diabetic rats. While L-arginine administration did not alter the increased TGF-β1 immunolocalization associated with diabetes, it significantly reduced total renal TGF-β1 levels. These findings suggest that total renal TGF-β1 levels decreased without changes in its immunolocalization. This difference can be attributed to methodological differences between the two techniques; while ELISA provides quantitative measurements of total tissue protein levels, immunohistochemistry primarily reflects protein localization and qualitative staining intensity. Consequently, qualitative immunohistochemical findings may not fully correlate with quantitative ELISA results, particularly during early-stage diabetic kidney changes where subtle decreases in total protein levels may not be easily detected by visual assessment. However, since this study represents an early stage of diabetic renal injury rather than advanced diabetic nephropathy, the observed changes reflect initial alterations in renal structure and TGF-β1 expression.

In conclusion, this study demonstrates that L-arginine administration reduces the increase in TGF-β1 levels in the kidneys associated with diabetes and partially improves early renal structural changes in an STZ-induced diabetic rat model. These findings indicate the potential protective role of L-arginine in the early stages of diabetic kidney damage. Further experimental studies, involving varying doses and treatment durations, along with detailed molecular analyses- including kidney histomorphometric analyses, receptor-binding studies, and detailed profiling of pro- and anti-inflammatory cytokines- are necessary to fully elucidate the protective effects and mechanisms of L-arginine against diabetic renal damage.

Peer-review: External, Independent.

Acknowledgements:
We would like to thank the Erciyes University Scientific Research Projects Unit for their support of this master thesis study under the project code TYL-2018-8378.

Declarations:

1. Statement of Originality:

As the authors of this manuscript, we hereby declare that the work presented is an original scholarly contribution solely prepared by us, and that it has not been copied, in whole or in part, from ant other work. All sources utilized in the study have been accurately and fully cited in accordance with acedemic and ethical standards. The manuscript has not been published previously and is not under simultaneous review by any other journal. We collectively assume full acedemic and ethical responsibilty for the content of the manuscript.

2. Author Contributions:

Concept: DYG; ***Conceptualization:*** DYG; ***Literature Search:*** DYG,AK; ***Data Collection:*** DYG,AK; ***Data Processing:*** DYG,AK; ***Analysis:*** DYG,AK,AA; ***Writing – original draft:*** DYG,AK; ***Writing – review & editing:*** DYG,AA.

3. Ethics approval:

This study was carried out after the animal experiment was approved Erciyes University Animal Experiments Local Ethics Committee (Date: 11.01.2018, Decision number: 18/017).

4. Funding/Support:
This research was supported within the scope of the project numbered TYL-2018-8378 by the Erciyes University Scientific Research Projects Coordination Unit.

5. Competing Interests:
The authors declare no competing interests.

6. GenAI Usage Statement:
No GenAI tools were used at any stage of the study.

7. Sustainable Development Goals:

REFERENCES

Adeva-Andany MM, Adeva-Contreras L, Fernández-Fernández C, Carneiro-Freire N, Domínguez-Montero A. Histological manifestations of diabetic kidney disease and its relationship with insulin resistance. Cur Diabetes Rev 2023; 19(1): 50-70.

Ajiboye BO, Shonibare MT, Oyinloye BE. Antidiabetic activity of watermelon (Citrullus lanatus) juice in alloxan-induced diabetic rats. J Diabetes Metab Disord 2020; 19(1): 343-52.

Bancroft J, Cook H. Manual of Histological Techniques. Churchill Living-stone; 1984.

Cakir S, Eren M, Senturk M, Sarica ZS. The effect of boron on some biochemical parameters in experimental diabetic rats. Biol Trace Elem Res 2018; 184(2): 165-72.

Chen C, Mitchell KD, Navar LG. Role of endothelium-derived nitricoxide in the renal hemodynamic response to amino acid infusion. Am J Physiol Regul Integr Comp Physiol 1992; 263(3): 510-6.

Crossmon G. A modification of Mallory's connective tissue stain with a discussion of the principles involved. Anat Rec 1937; 69: 33-8.

Dedoussis GVZ, Kaliora AC, Panagiotakos DB. Genes, diet and type 2 diabetes mellitus: a review. Rev Diabet Stud 2007; 4(1): 13.

Ejrnaes M, Von Herrath MG, Christen U. Cure of chronic viral infection and virus-induced type 1 diabetes by neutralizing antibodies. Clin Exp Immunol 2006; 13(2-4): 337-47.

El-Missiry MA, Othman AI, Amer MA. L-Arginine ameliorates oxidative stress in alloxan induced experimental diabetes mellitus. J Appl Toxicol 2004; 24(2): 93-7.

Gram A, Grazul-Bilska AT, Boos A, Rahman NA, Kowalewski MP. Lipopolysaccharide disrupts gap junctional intercellular communication in an immortalized ovine luteal endothelial cell line. Toxicol in Vito 2019; 60(5): 437-49.

Heydarpour F, Sajadimajd S, Mirzarazi E, Haratipour P, Joshi T, Farzaei MH, Khan H, Echeverría J. Involvement of TGF-β and autophagy pathways in pathogenesis of diabetes: a comprehensive review on biological and pharmacological insights. Front Pharmacol 2020; 11: 498758.

Hill C, Flyvbjerg A, Gronbaek H, Petrik J, Hill DJ, Thomas CR, Sheppard MC, Logan A. The renal expression of transforming growth factor-β isoforms and their receptors in acute and chronic experimental diabetes in rats. Endocrinol 2000; 141(3): 1196-208.

Hoogeveen EK. The epidemiology of diabetic kidney disease. Kidney Dial 2022; 2(3): 433-42.

IDF Diabetes Atlas-11th Edition 2025. https://diabetesatlas.org/atlas/tenth-edition/; Accessed Date:11.09.2025.

Kato M, Yuan H, Xu ZG, Lanting L, Li SL, Wang M, Hu MCT, Reddy MA, Natarajan R. Role of the Akt/FoxO3a pathway in TGF-β1 mediated mesangial cell dysfunction: a novel mechanism related to diabetic kidney disease. J Am Soc Nephrol 2006; 17(12): 3325-35.

Katoh T, Takahashi K, Klahr S, Reyes AA, Badr KF. Dietary supplementation with L-arginine ameliorates glomerular hypertension in rats with subtotal nephrectomy. J Am Soc Nephrol 1994; 4(9): 1690-4.

Kawano H, Motoyama T, Hirai N, Kugiyama K, Yasue H, Ogawa H. Endothelial dysfunction in hypercholesterolemia is improved by L-arginine administration: possible role of oxidative stress. Atherosclerosis 2002; 161(2): 375-80.

Kaya NK, Eren M, Şentürk M, Soyer Sarıca Z. The effects of magnesium and L-carnitine on some biochemical parameters in experimental diabetic rats. Appl Biol Res 2022; 16(3): 456-70.

Klahr S, Morrissey J. L-arginine as a therapeutic tool in kidney disease. Semin Nephrol 2004; 24(4): 389-94.

Koszegi S, Molnar A, Lenart L, Hodrea J, Balogh DB, Lakat T, Szkibinszkij E, Hosszu A, Sparding N, Genovese F, Wagner L, Vannay A, Szabo AJ, Fekete A. RAAS inhibitors directly reduce diabetes-induced renal fibrosis via growth factor inhibition. J Physiol 2019; 597(1): 193-209.

Küçük M, Çevik A, Emre A. Deneysel Pankreas Transplantasyonu. Experimental Pancreas Transplantation. Deneysel Tıp araştırma Enstitüsü Dergisi. 2012; 2(3): 3-10.

Ito K, Chen J, Seshan SV, Khodadadian JJ, Gallagher R, Chaar ME, Felsen D. Dietary arginine supplementation attenuates renal damage after relief of unilateral ureteral obstruction in rats. Kidney Int 2005; 68(2): 515-28.

Lenzen S. The mechanisms of alloxan-and streptozotocin-induced diabetes. Diabetologia 2008; 51(2): 216-26.

Luna LG. Manual of Histologic Staining Methods of the Armed Forces Institute of Pathology. Third Edition. New York: Blakiston Division,1968; p.34-75.

Mistry J, Biswas M, Sarkar S, Ghosh S. Antidiabetic activity of mango peel extract and mangiferin in alloxan-induced diabetic rats. Future J Pharm Sci 2023; 9(1): 22.

Müller G. Methods to induce experimental diabetes mellitus. Hock F. eds. In: Drug Discovery and Evaluation: Pharmacological Assays. Springer Cham 2016; pp.2569-81.

Noris M, Remuzzi G. Physiology and pathophysiology of nitric oxide in chronic renal disease. Proc Assoc Am Physicians 1999; 111(6): 602-10.

Palsamy P, Subramanian S. Resveratrol protects diabetic kidney by attenuating hyperglycemia-mediated oxidative stress and renal inflammatory cytokines via Nrf2-Keap1 signaling. Biochim Biophys Acta Mol Basis Dis 2011; 1812(7): 719-31.

Pieper GM, Peltier BA. Amelioration by L-arginine of dysfunctional arginine/nitric oxide pathway in diabetic endothelium. J Cardiovasc Pharmacol 1995; 25(3): 397-403.

Rees DA, Alcolado JC. Animal models of diabetes mellitus. Diabet Med 2005; 22(4): 359-70.

Reeves WB, Andreoli TE. Transforming growth factor β contributes to progressive diabetic nephropathy. Proc Natl Acad Sci USA 2000; 97(14): 7667-9.

Reyes AA, Porras BH, Chasalow FI, Klahr S. L-arginine decreases the infiltration of the kidney by macrophages in obstructive nephropathy and puromycin-induced nephrosis. Kidney Int 1994; 45(5): 1346-54.

Roy S, Ahmed F, Banerjee S, Saha U. Naringenin ameliorates streptozotocin-induced diabetic rat renal impairment by downregulation of TGF-β1 and IL-1 via modulation of oxidative stress correlates with decreased apoptotic events. Pharm Biol 2016; 54(9): 1616-27.

Sadik NA. L-arginine attenuates diabetic nephropathy in streptozotocin-induced diabetic rats. Egypt Jl Biochem Mol Biol 2008; 26(1): 1-22.

Saleh S, El-Demerdash E. Protective effects of L-arginine against cisplatin-induced renal oxidative stress and toxicity: Role of nitric oxide. Basic Clin Pharmacol Toxicol 2005; 97(2): 91-7.

Sayed MM, Abd el-Rady NM, Gomaa WM, Hosny A, Gomaa AM. Antioxidant, antiapoptotic, and antifibrotic abilities of L-Arginine ameliorate the testicular dysfunction in diabetic rats. Tissue Cell 2023; 82: 102036.

Schneider CA, Rasband WS, Eliceiri KW. NIH Image to ImageJ: 25 years of image analysis. Nat Methods 2012; 9(7): 671-5.

Sharma K, Ziyadeh FN. Renal hypertrophy is associated with upregulation of TGF-beta 1 gene expression in diabetic BB rat and NOD mouse. Am J Physiol Renal Physiol 1994; 267(6): 1094-101.

Szhudelski T. The mechanism of alloksan and STZ action in β cells of rat pancreas. Physiol Res 2001; 50(6): 536-46.

Szlas A, Kurek JM, Krejpcio Z. The potential of L-arginine in prevention and treatment of disturbed carbohydrate and lipid metabolism-a review. Nutrients 2022; 14(5): 961.

Talakatta G, Sarikhani M, Muhamed J, Dhanya K, Somashekar BS, Mahesh PA, Sundaresan N, Ravindra PV. Diabetes induces fibrotic changes in the lung through the activation of TGF-β signaling pathways. Sci Rep 2018; 8(1): 11920.

Tarladacalisir YT, Kanter M, Uygun M. Protective effects of vitamin C on cisplatin-induced renal damage: a light and electron microscopic study. Ren Fail 2008; 30(1): 1-8.

Wang CH, Li F, Hiller S, Kim HS, Maeda N, Smithies O, Takahashi N. A modest decrease in endothelial NOS in mice comparable to that associated with human NOS3 variants exacerbates diabetic nephropathy. Proc Natl Acad Sci USA 2011; 108(5): 2070-5.

Yaman Gram D, Şentürk M, Özocak GK, Doğan ND, Ekebaş G, Atasever A, Eren M. Effect of dietary L-arginine supplementation on the expression of vascular endothelial growth factor A, its receptors, and nitric oxide system components in the pancreas of streptozotocin-induced diabetic rats. Tissue Cell 2025; 103072.

Yang Y, Xu G. Update on pathogenesis of glomerular hyperfiltration in early diabetic kidney disease. Front Endocrinol 2022; 13, 872-918.

Yılmaz MT. Tip 1 diabetes mellitus. İmamoğlu Ş. eds. In: Diabetes Mellitus. İstanbul: Deomed Medikal Yayıncılık, 2006; pp:55-66.

You H, Gao T, Cooper TK, Morris Jr SM, Awad AS. Diabetic nephropathy is resistant to oral L-arginine or L-citrulline supplementation. Am J Physiol Renal Physiol 2014; 307(11): 1292-301.

Zhang C, Xue S, Ren P, Han S, Zhou Y, Si Y, Shang L. Advances in the epigenetic mechanisms of diabetic

nephropathy pathogenesis. Diabetes Metab Syndr Obes 2025; 2629-39.

Ziyadeh FN, Han DC, Cohen JA, Guo J, Cohen MP. Glycated albümin stimulates fibronectin gene expression in glomerular mesangial cells: Involvement of the transforming growth factor-β system. Kidney Int 1998; 53(3): 631-8.

Ziyadeh FN. The extracellular matrix in diabetic nephropathy. Am J Kidney Dis 1993; 22(5): 736-44.